The Plant Cell, Vol. 27: 620–632, March 2015, www.plantcell.org

Transcription Factors SOD7/NGAL2 and DPA4/NGAL3 Act Redundantly to Regulate Seed Size by Directly Repressing *KLU* Expression in *Arabidopsis thaliana*

Yueying Zhang,[a,b] Liang Du,[a,1] Ran Xu,[a] Rongfeng Cui,[a] Jianjun Hao,[c] Caixia Sun,[c] and Yunhai Li[a,2]

[a] State Key Laboratory of Plant Cell and Chromosome Engineering, Institute of Genetics and Developmental Biology, Chinese Academy of Sciences, Beijing 100101, China

[b] University of Chinese Academy of Sciences, Beijing 100039, China

[c] College of Life and Health Sciences, Northeastern University, Shenyang 110004, China

ORCID ID: 0000-0002-0025-4444 (Y.L.)

Although seed size is one of the most important agronomic traits in plants, the genetic and molecular mechanisms that set the final size of seeds are largely unknown. We previously identified the ubiquitin receptor DA1 as a negative regulator of seed size, and the *Arabidopsis thaliana da1-1* mutant produces larger seeds than the wild type. Here, we describe a B3 domain transcriptional repressor NGATHA-like protein (NGAL2), encoded by the suppressor of *da1-1* (*SOD7*), which acts maternally to regulate seed size by restricting cell proliferation in the integuments of ovules and developing seeds. Overexpression of *SOD7* significantly decreases seed size of wild-type plants, while the simultaneous disruption of *SOD7* and its closest homolog *DEVELOPMENT-RELATED PcG TARGET IN THE APEX4* (*DPA4*/*NGAL3*) increases seed size. Genetic analyses indicate that SOD7 and DPA4 act in a common pathway with the seed size regulator KLU to regulate seed growth, but do so independently of DA1. Further results show that SOD7 directly binds to the promoter of *KLUH* (*KLU*) in vitro and in vivo and represses the expression of *KLU*. Therefore, our findings reveal the genetic and molecular mechanisms of *SOD7*, *DPA4*, and *KLU* in seed size regulation and suggest that they are promising targets for seed size improvement in crops.

INTRODUCTION

Seed size is an important agronomic trait and is also a key ecological trait that influences many aspects of a species' regeneration strategy, such as seedling survival rates and seed dispersal syndrome (Harper et al., 1970; Westoby et al., 2002; Moles et al., 2005; Fan et al., 2006; Orsi and Tanksley, 2009; Gegas et al., 2010). In higher plants, seed development starts with a double fertilization process, in which one of the two haploid pollen nuclei fuses with the haploid egg cell to produce the diploid embryo, while the other sperm nucleus fuses with the diploid central cell to form the triploid endosperm (Lopes and Larkins, 1993). The integuments surrounding the ovule are maternal tissues and form the seed coat after fertilization. Therefore, seed size is determined by the growth of the embryo, the endosperm, and the maternal tissues. However, the genetic and molecular mechanisms setting the limits of seed growth are almost unknown in plants.

Several factors that function maternally to regulate seed size have been identified in *Arabidopsis thaliana*. For example, TRANSPARENT TESTA GLABRA2 (TTG2) influences seed growth by increasing cell elongation in the maternal integuments (Garcia et al., 2005; Ohto et al., 2009), while APETALA2 (AP2) may regulate seed growth by limiting cell elongation in the maternal integuments (Jofuku et al., 2005; Ohto et al., 2005, 2009). By contrast, AUXIN RESPONSE FACTOR2 (ARF2) acts maternally to control seed growth by restricting cell proliferation (Schruff et al., 2006). Similarly, the ubiquitin receptor DA1 acts synergistically with the E3 ubiquitin ligases DA2 and EOD1/BB to regulate seed size by limiting cell proliferation in the maternal integuments (Li et al., 2008; Xia et al., 2013). Mutations in the suppressor of *da1-1* (*SOD2*), which encodes the ubiquitin-specific protease (UBP15), suppress the large seed phenotype of *da1-1* (Du et al., 2014). DA1 physically associates with UBP15/SOD2 and modulates the stability of UBP15. These studies show that the ubiquitin pathway plays an important part in the maternal control of seed size. KLU/CYTOCHROME P450 78A5 (CYP78A5) regulates seed size by increasing cell proliferation in the maternal integuments of ovules (Adamski et al., 2009). KLU has also been suggested to generate mobile plant growth substances that promote cell proliferation (Anastasiou et al., 2007; Adamski et al., 2009). By contrast, overexpression of *CYP78A6*/*EOD3* increases both cell proliferation and cell elongation in the integuments, resulting in large seeds (Fang et al., 2012). Seed size is also determined by zygotic tissues. Several factors have been described to influence seed size via the zygotic tissues in Arabidopsis, including HAIKU1 (IKU1), IKU2, MINISEED3 (MINI3), and SHORT HYPOCOTYL UNDER BLUE1 (SHB1) (Garcia et al., 2003; Luo et al., 2005; Zhou et al., 2009; Wang et al., 2010; Kang et al., 2013). *iku* and *mini3* mutants form small seeds due to precocious cellularization of the endosperm (Garcia et al., 2003; Luo et al., 2005; Wang et al., 2010). SHB1 associates with *MINI3* and

[1] Current address: College of Biological Sciences and Biotechnology, Beijing Forestry University, Beijing, 100083, China.

[2] Address correspondence to yhli@genetics.ac.cn.

The author responsible for distribution of materials integral to the findings presented in this article in accordance with the policy described in the Instructions for Authors (www.plantcell.org) is: Yunhai Li (yhli@genetics.ac.cn).

www.plantcell.org/cgi/doi/10.1105/tpc.114.135368

IKU2 promoters and regulates expression of *MINI3* and *IKU2* (Zhou et al., 2009; Kang et al., 2013). ABA INSENSITIVE5 was recently described to repress the expression of *SHB1* (Cheng et al., 2014), and MINI3 was reported to activate the expression of the cytokinin oxidase (*CKX2*) (Li et al., 2013), suggesting that phytohormones regulate endosperm growth. In addition, endosperm growth is influenced by parent-of-origin effects (Scott et al., 1998; Xiao et al., 2006).

To understand the genetic and molecular mechanisms of seed size control, we identified modifiers of the large seed phenotype of *da1-1* through an activation-tagging screen (Fang et al., 2012). Here, we describe a suppressor of *da1-1* (*sod7-1D*), which forms smaller seeds than *da1-1*. *SOD7* encodes a B3 domain transcriptional repressor NGAL2. Overexpression of *SOD7* dramatically decreases seed size of wild-type plants, whereas the simultaneous disruption of *SOD7* and its closest homolog *DEVELOPMENT-RELATED PcG TARGET IN THE APEX4* (*DPA4*)/*NGAL3* causes large seeds. Genetic analyses show that *SOD7* and *DPA4* act in a common pathway with *KLU* to regulate seed size, but do so independently of *DA1*. Further results reveal that SOD7 directly binds to the *KLU* promoter and represses expression of *KLU*. Thus, our findings identify SOD7 and DPA4 as negative regulators of seed size and define the genetic and molecular mechanisms of SOD7, DPA4, and KLU in seed size control.

RESULTS

sod7-1D Suppresses the Seed Size Phenotype of *da1-1*

We previously identified the ubiquitin receptor DA1 as a negative regulator of seed size in Arabidopsis (Li et al., 2008). The *da1-1* mutant formed large seeds due to increased cell proliferation in the maternal integuments (Li et al., 2008; Xia et al., 2013). To identify additional factors that influence seed size, we initiated a T-DNA activation-tagging screen for modifiers of *da1-1* (Fang et al., 2012). A dominant *sod7-1D* was isolated from seeds produced from ~16,000 T1 plants (Figure 1A). Seeds of the *sod7-1D da1-1* double mutant were significantly smaller and lighter than *da1-1* seeds (Figures 1A, 1E, and 1F). The embryo constitutes the major volume of a mature seed in Arabidopsis. *sod7-1D da1-1* embryos were smaller than *da1-1* embryos (Figure 1B). The size of *sod7-1D da1-1* cotyledons was significantly reduced compared with that of *da1-1* cotyledons (Figure 1G). In addition, the *sod7-1D da1-1* double mutant formed smaller leaves and flowers than *da1-1* (Figures 1C, 1D, 1H, and 1I). Thus, the *sod7-1D* mutation suppressed the seed and organ size phenotypes of *da1-1*.

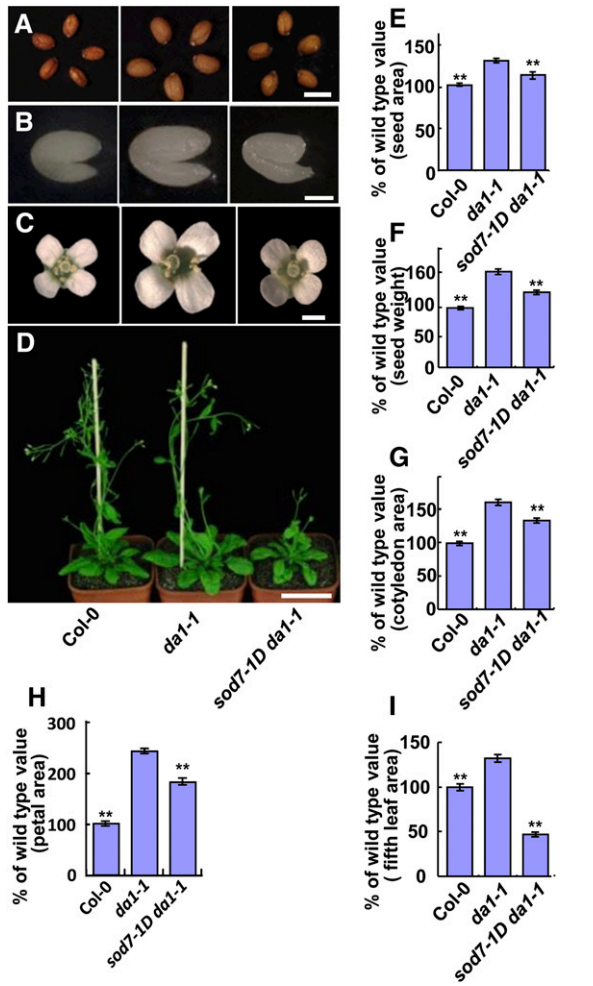

Figure 1. Isolation of a Suppressor of *da1-1* (*sod7-1D*).

(A) to **(D)** Seeds **(A)**, mature embryos **(B)**, flowers **(C)**, and 30-d-old plants **(D)** of the wild type, *da1-1*, and *sod7-1D da1-1* (from left to right).
(E) Seed area of the wild type, *da1-1*, and *sod7-1D da1-1* (n = 100).
(F) Seed weight of the wild type, *da1-1*, and *sod7-1D da1-1*. The weights of five sample batches were measured for each seed lot (n = 5).
(G) Cotyledon area of 10-d-old wild-type, *da1-1*, and *sod7-1D da1-1* seedlings (n = 20).
(H) and **(I)** Petal area and the fifth leaf area of Col-0, *da1-1*, and *sod7-1D da1-1*. Fifty petals and eight leaves were used to measure petal area and the fifth leaf area, respectively.
Values in **(E)** to **(I)** are given as mean ± SE relative to the respective wild-type values, set at 100%. **P < 0.01 compared with *da1-1* (Student's t test). Bars = 0.5 mm in **(A)**, 0.2 mm in **(B)**, 1 mm in **(C)**, and 5 cm in **(D)**.

sod7-1D Produces Small Seeds

We isolated the single *sod7-1D* mutant among F2 progeny derived from a cross between the wild type (Columbia-0 [Col-0]) and *sod7-1 D da1-1*. The *sod7-1D* seeds were significantly smaller and lighter than wild-type seeds (Figures 2A, 2B, 2G, and 2H). We further isolated and visualized embryos from mature wild-type and *sod7-1D* seeds. The *sod7-1D* embryos were smaller than wild-type embryos (Figures 2C and 2D). The changes in seed size were also reflected in the size of seedlings (Figures 2E and 2F). The 10-d-old *sod7-1D* cotyledons were significantly smaller than wild-type cotyledons (Figure 2E, 2F, and 2I). In addition, the *sod7-1D* mutants exhibited small leaves and flowers compared with the wild type (Supplemental Figures 1A to 1D). The decreased size of *sod7-1D* leaves and petals was not caused by smaller cells (Supplemental Figures 1E and 1F), indicating that the *sod7-1D* mutation results in a decrease in cell number. In fact, the average area of epidermal cells in *sod7-1D* petals was larger than that in wild-type petals (Supplemental Figure 1E), suggesting a possible compensation mechanism between cell number and cell size.

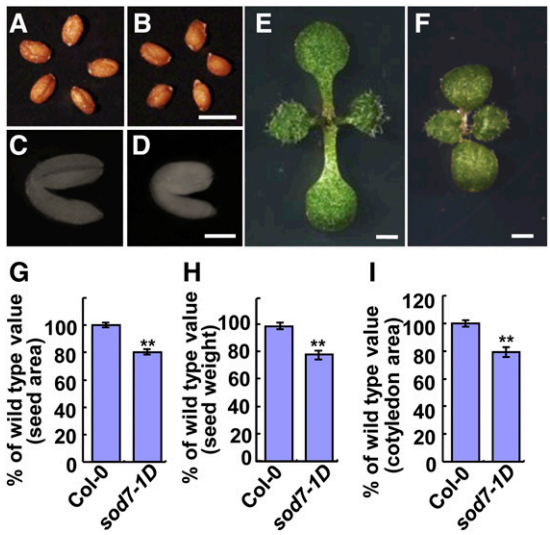

Figure 2. Seed and Organ Size in the *sod7-1D* Mutant.

(A) and **(B)** Seeds of Col-0 **(A)** and *sod7-1D* **(B)**.
(C) and **(D)** Mature embryos of Col-0 **(C)** and *sod7-1D* **(D)**.
(E) and **(F)** Ten-day-old seedlings of Col-0 **(E)** and *sod7-1D* **(F)**.
(G) Seed area of Col-0 and *sod7-1D* (n = 120).
(H) Seed weight of Col-0 and *sod7-1D*. The weights of five sample batches were measured for each seed lot (n = 5).
(I) Cotyledon area of 10-d-old Col-0 and *sod7-1D* seedlings (n = 20).
Values in **(G)** to **(I)** are given as mean ± SE relative to the respective wild-type values, set at 100%. **P < 0.01 compared with the wild type (Student's t test). Bars = 0.5 mm in **(A)** and **(B)**, 0.2 mm in **(C)** and **(D)**, and 1 mm in **(E)** and **(F)**.

SOD7 Encodes a B3 Domain Transcriptional Repressor NGAL2

To determine whether the seed and organ size phenotypes of *sod7-1D* were caused by the T-DNA insertion, we first analyzed the genetic linkage of the mutant phenotypes with Basta resistance, which is conferred by the selectable marker of the activation-tagging vector (Fan et al., 2009). In a T2 population, 181 plants with *sod7-1D da1-1* phenotypes were resistant, whereas 55 plants with *da1-1* phenotypes were sensitive, indicating that the insertion cosegregates with the *sod7-1D* phenotypes. To clone *SOD7*, we isolated the T-DNA flanking sequences using thermal asymmetric interlaced PCR (TAIL-PCR; Liu et al., 1995). DNA sequencing revealed that the T-DNA had inserted ~5.6 kb upstream of At3g11580 and ~3.7 kb upstream of At3g11590 gene (Figure 3A). To determine which gene is responsible for the *sod7-1D* phenotypes, we examined the mRNA levels of these two genes. The mRNA of At3g11590 accumulated at a similar level in *sod7-1D da1-1* and *da1-1*, suggesting that At3g11590 is not the *SOD7* gene (Figure 3B). By contrast, the expression level of At3g11580 in *sod7-1D da1-1* plants was dramatically higher than that in *da1-1* plants, suggesting that At3g11580 is the *SOD7* gene (Figure 3B). To further confirm whether the *sod7-1D* phenotypes were caused by ectopic At3g11580 expression, we overexpressed the At3g11580 gene (*35S:GFP-SOD7*) in wild-type plants (Col-0) and isolated 37 transgenic plants. Most transgenic lines had small seeds and organs (Figures 3D to 3F; Supplemental Figure 2), similar to those observed in the *sod7-1D* single mutant, indicating that At3g11580 is the *SOD7* gene.

SOD7 encodes a NGATHA-like protein (NGAL2) containing a B3 DNA binding domain and a transcriptional repression motif (Figure 3C) (Alvarez et al., 2009; Ikeda and Ohme-Takagi, 2009; Trigueros et al., 2009). *SOD7* belongs to the *RAV* (*RELATED TO ABI3 AND VP1*) gene family that consists of 13 members in Arabidopsis (Supplemental Figure 3 and Supplemental Data Set 1) (Swaminathan et al., 2008). Several members of the RAV family contain the putative transcriptional repression motifs, including NGA1, NGA2, NGA3, NGA4, NGAL1, NGAL2/SOD7, and NGAL3 (Supplemental Figure 3) (Ikeda and Ohme-Takagi, 2009). The transcriptional repression motifs in NGA1, NGAL1, and NGAL2/SOD7 have been shown to possess repressive activity (Ikeda and Ohme-Takagi, 2009), indicating that they are transcriptional repressors. SOD7 exhibits the highest similarity to Arabidopsis NGAL3/DPA4 (Supplemental Figure 3), which is an established regulator of leaf serrations (Engelhorn et al., 2012), but no previously identified function in seed size control.

Expression Pattern and Subcellular Localization of *SOD7*

To monitor *SOD7* expression pattern during development, the *ProSOD7:GUS* and *ProSOD7:SOD7-GFP* vectors were constructed and transformed into wild-type plants, respectively. The tissue-specific expression patterns of *SOD7* were examined using a histochemical assay for GUS activity. In seedlings, relatively higher GUS activity was detected in younger leaves than in older leaves (Figures 4A to 4C). In flowers, GUS activity was observed in sepals, petals, stamens, and carpels (Figures 4D to 4K). GUS activity was stronger in younger floral organs than in older ones (Figures 4D to 4K). Expression of *SOD7* was also detected in the nucellus, inner integuments, and outer integuments of developing ovules (Figures 4L to 4O). Thus, these results are consistent with the function of *SOD7* in cell proliferation.

As *SOD7* encodes a B3 domain transcriptional repressor, we speculated that SOD7 is localized in the nucleus. To determine subcellular localization of SOD7, we expressed a GFP-SOD7 fusion protein under the control of the 35S promoter in wild-type plants. Transgenic lines overexpressing *GFP-SOD7* formed smaller seeds than the wild type (Figure 3D), indicating that the GFP-SOD7 fusion protein is functional. As shown in Figures 4P and 4Q and Supplemental Figures 4D to 4I, GFP fluorescence in *Pro35S:GFP-SOD7* transgenic plants was observed exclusively in nuclei. We further transformed *sod7-2 dpa4-3* plants with *ProSOD7:SOD7-GFP*. Transgenic plants produced smaller seeds and petals than *sod7-2 dpa4-3*, indicating that the SOD7-GFP protein is functional (Supplemental Figures 4A and 4B). Interestingly, transgenic lines had significant increases in *SOD7* mRNA compared with wild-type plants (Supplemental Figure 4C). It is possible that the integration regions of transgenes in the genome affect the promoter activity of *ProSOD7:SOD7-GFP* because these transgenic lines contain one copy of the transgene (Supplemental Figure 4). We further observed GFP florescence in *ProSOD7:SOD7-GFP* transgenic plants. As shown in Figures 4P to 4S and Supplemental Figures 4D to 4I, GFP signal was only detected in nuclei. Thus, these results show that SOD7 is a nuclear-localized protein.

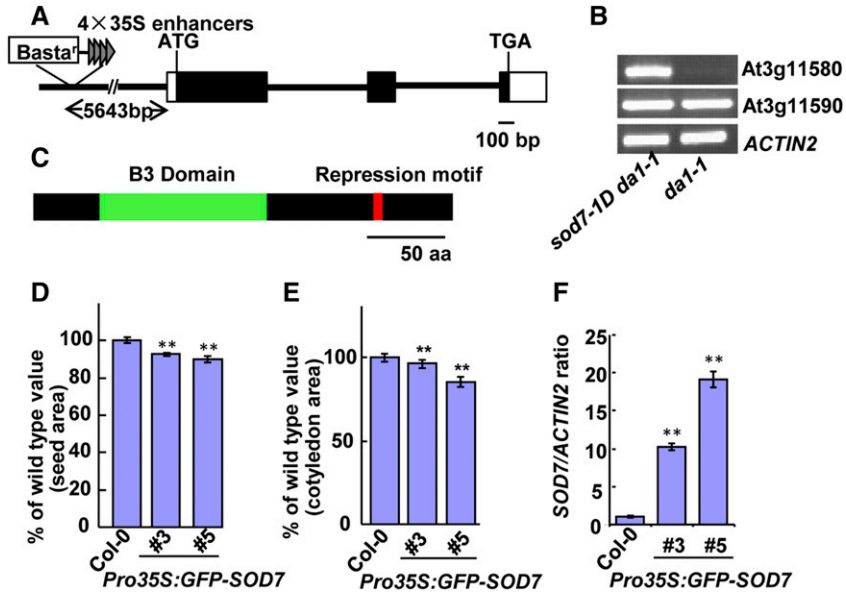

Figure 3. Cloning of *SOD7*.

(A) Structure of the T-DNA insertion in the *sod7-1D* mutant.
(B) Expression levels of At3g11580 (*SOD7*) and At3g11590 in *da1-1* and *sod7-1D da1-1* seedlings as determined by RT-PCR. Three independent experiments were performed with similar results.
(C) SOD7 contains a B3 DNA binding domain (green) and a transcriptional repression motif (red).
(D) Seed area of Col-0, *35S:GFP-SOD7#3*, and *35S:GFP-SOD7#5* (n = 120).
(E) Cotyledon area of 10-d-old Col-0, *35S:GFP-SOD7#3*, and *35S:GFP-SOD7#5* seedlings (n = 20).
(F) Expression levels of *SOD7* in Col-0, *35S:GFP-SOD7#3*, and *35S:GFP-SOD7#5* seedlings. Means were calculated from three biological samples (n = 3). Values in **(D)** to **(F)** are given as mean ± SE relative to the respective wild-type values, set at 100%. **P < 0.01 compared with the wild type (Student's t test).

SOD7/NGAL2 Acts Redundantly with *DPA4/NGAL3* to Regulate Seed Size

To further investigate the function of *SOD7* in seed size control, we isolated dSpm transposon insertional loss-of-function mutants for *SOD7* and *DPA4/NGAL3*, the most closely related family member. *sod7-2* (SM_3.34191) was identified with a dSpm transposon insertion in the first exon of the *SOD7* gene (Figure 5A). *dpa4-3* (SM_3.36641) had a dSpm transposon insertion in the first exon of *DPA4/NGAL3* (Figure 5B). The dSpm transposon insertion sites were confirmed by PCR and sequencing PCR products (Supplemental Figures 5A and 5B). *sod7-2* and *dpa4-3* mutants had no detectable full-length transcripts of *SOD7* and *DPA4* (Supplemental Figures 5C and 5D), respectively.

Seeds from *sod7-2* and *dpa4-3* mutants were slightly larger and heavier than seeds from wild-type plants (Figures 5C, 5G, and 5H). The cotyledon area of *sod7-2* and *dpa4-3* mutants was increased compared with that of the wild type (Figure 5I). Considering that SOD7 shares the highest similarity with DPA4, we speculated that SOD7 may act redundantly with DPA4 to influence seed size. To test this, we generated the *sod7-2 dpa4-3* double mutant. As shown in Figures 5C, 5D, 5G, and 5H, the seed size and weight phenotypes of the *sod7-2* mutant were synergistically enhanced by the disruption of *DPA4*, indicating that *SOD7* functions redundantly with *DPA4* to regulate seed size. We further measured the cotyledon area of 10-d-old seedlings. A synergistic enhancement of cotyledon size of *sod7-2* by the *dpa4-3* mutation was also observed (Figure 5I). In addition, the *sod7-2 dpa4-3* double mutant formed larger leaves and flowers than their parental lines (Figures 5E and 5F; Supplemental Figure 6). The flowering time of the *sod7-2 dpa4-3* double mutant was similar to that of the wild type (Supplemental Figure 7). Thus, these results indicate that *SOD7* and *DPA4* act redundantly to control seed and organ growth.

SOD7 and *DPA4* Act Maternally to Regulate Seed Size

As the size of a seed is determined by the zygotic and/or maternal tissues (Garcia et al., 2005; Xia et al., 2013; Du et al., 2014), we asked whether *SOD7* and *DPA4* function maternally or zygotically. We therefore performed reciprocal cross experiments between the wild type and *sod7-2 dpa4-3*. The effect of *sod7-2 dpa4-3* on seed size was observed only when *sod7-2 dpa4-3* was used as maternal plants (Figure 6A). The size of seeds from *sod7-2 dpa4-3* plants pollinated with wild-type pollen was similar to that from self-pollinated *sod7-2 dpa4-3* plants (Figure 6A). By contrast, the size of seeds from wild-type plants pollinated with *sod7-2 dpa4-3* mutant pollen was similar to that from the self-pollinated wild-type plants (Figure 6A). These results indicate that *sod7-2 dpa4-3* acts maternally to influence seed size. We further investigated the size of Col-0/Col-0 F2, Col-0/*sod7-2 dpa4-3* F2, *sod7-2 dpa4-3*/Col-0 F2, and *sod7-2 dpa4-3*/*sod7-2 dpa4-3* F2 seeds. As shown in Figure 6B, *sod7-2 dpa4-3*/ *sod7-2 dpa4-3* F2 seeds were larger than wild-type seeds, while the size of Col-0/*sod7-2 dpa4-3* F2 and *sod7-2 dpa4-3*/Col-0 F2 seeds was similar to that of wild-type seeds. Thus, these results

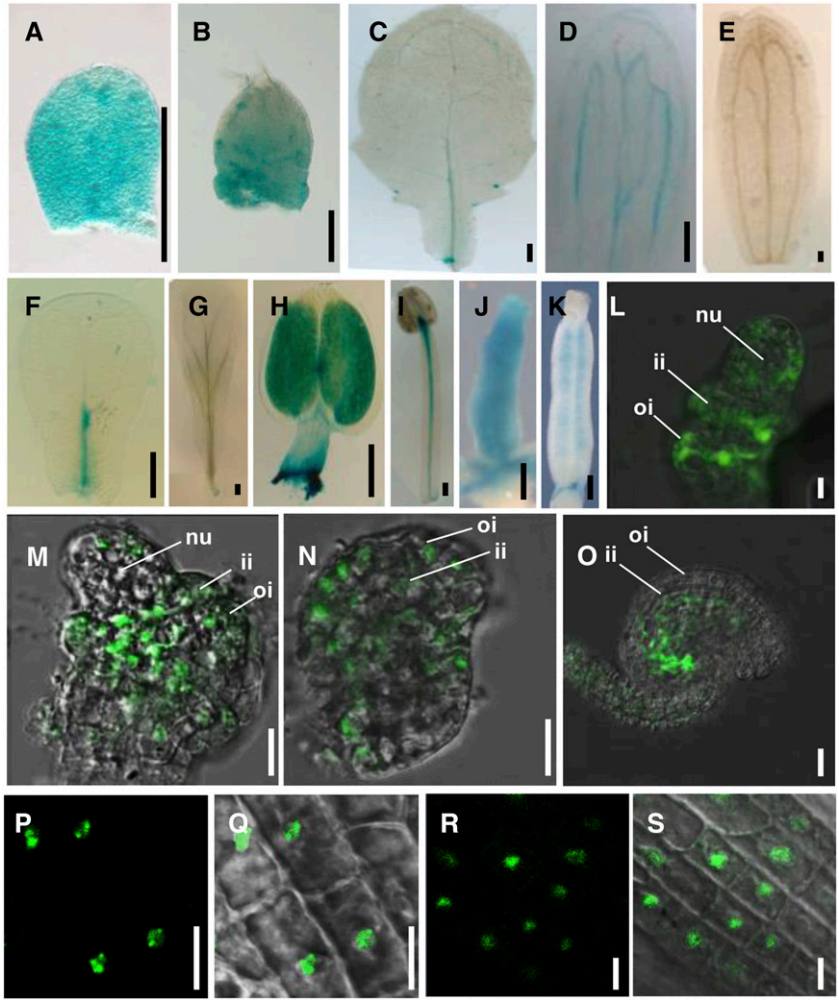

Figure 4. Expression Pattern and Subcellular Localization of *SOD7*.

(A) to **(K)** *SOD7* expression activity was monitored by *pSOD7:GUS* transgene expression. Histochemical analysis of GUS activity in the developing leaves (**[A]** to **[C]**), the developing sepals (**[D]** and **[E]**), the developing petals (**[F]** and **[G]**), the developing stamens (**[H]** and **[I]**), and the developing carpels (**[J]** and **[K]**). Gynoecia in **(J)** and **(K)** are in flower stage 9 and 11, respectively.
(L) to **(O)** GFP florescence of SOD7-GFP in developing ovules of *ProSOD7:SOD7-GFP* transgenic plants. oi, the outer integument; ii, the inner integument; nu, nucellus.
(P) and **(Q)** GFP fluorescence of SOD7-GFP in roots of *Pro35S:GFP-SOD7* transgenic plants.
(R) and **(S)** GFP florescence of SOD7-GFP in roots of *ProSOD7:SOD7-GFP* transgenic plants.
Bars = 100 μm in **(A)** to **(K)**, 10 μm in **(L)** to **(N)**, 20 μm in **(O)**, and 25 μm in **(P)** to **(S)**.

indicate that the embryo and endosperm genotypes for *SOD7* and *DPA4* do not determine seed size, and *SOD7* and *DPA4* are required in the sporophytic tissue of the mother plant to control seed growth.

SOD7 and *DPA4* Regulate Cell Proliferation in the Maternal Integuments

The reciprocal crosses showed that *SOD7* and *DPA4* function maternally to influence seed size. The integuments surrounding the ovule are maternal tissues, which could set the growth potential of the seed coat after fertilization. Consistent with this idea, several studies showed that the integument size influences the final size of seeds in Arabidopsis (Garcia et al., 2005; Schruff et al., 2006; Adamski et al., 2009; Xia et al., 2013; Du et al., 2014). We therefore asked whether *SOD7* acts through the maternal integuments to determine seed size. To test this, we characterized mature ovules of the wild type and *sod7-2 dpa4-3*. As shown in Figures 6C and 6D, the *sod7-2 dpa4-3* ovules were obviously larger than wild-type ovules. The outer integument length of *sod7-2 dpa4-3* ovules was significantly increased compared with that of wild-type ovules (Figure 6E).

As the size of the integument is determined by cell proliferation and cell expansion, we examined the number and size of outer integument cells in wild-type and *sod7-2 dpa4-3* ovules. As shown in Figure 6F, the number of outer integument cells in *sod7-2 dpa4-3* ovules was increased compared with that in wild-type ovules. By contrast, the length of outer integument cells in *sod7-2 dpa4-3*

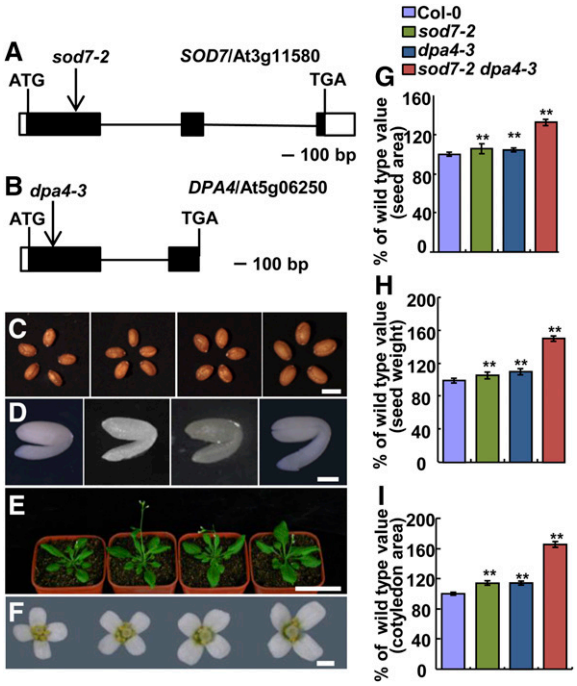

Figure 5. *SOD7* Acts Redundantly with *DPA4* to Regulate Seed Size.

(A) *SOD7* gene structure. The start codon (ATG) and the stop codon (TGA) are shown. Closed boxes indicate the coding sequence, and the lines between boxes indicate introns. The dSpm transposon insertion site (*sod7-2*) in *SOD7* is indicated.

(B) *DPA4/NGAL3* gene structure. The start codon (ATG) and the stop codon (TGA) are shown. Closed boxes indicate the coding sequence, and the line between boxes indicates intron. The dSpm transposon insertion site (*dpa4-3*) in *NGAL3* is indicated.

(C) to **(F)** Seeds **(C)**, mature embryos **(D)**, 25-d-old plants **(E)**, and flowers **(F)** of Col-0, *sod7-2*, *dpa4-3*, and *sod7-2 dpa4-3* (from left to right).

(G) and **(H)** Seed area **(G)** and seed weight **(H)** of Col-0, *sod7-2*, *dpa4-3*, and *sod7-2 dpa4-3*. One hundred and twenty seeds were used to measure seed area (n = 120). The weights of five sample batches were measured for each seed lot (n = 5).

(I) Cotyledon area of Col-0, *sod7-2*, *dpa4-3*, and *sod7-2 dpa4-3* seedlings (n = 20).

Values in **(G)** to **(I)** are given as mean ± SE relative to the respective wild-type values, set at 100%. **P < 0.01 compared with the wild type (Col-0) (Student's t test). Bars = 0.5 mm in **(C)**, 0.2 mm in **(D)**, 5 cm in **(E)**, and 1 mm in **(F)**.

ovules was similar to that in wild-type ovules (Figure 6G). These results showed that *SOD7* is required for cell proliferation in the maternal integuments of ovules. After fertilization, cells in the integument mainly undergo expansion but still divide. We further examined the number and size of outer integument cells in wild-type and *sod7-2 dpa4-3* seeds at 6 and 8 d after pollination (DAP). In wild-type seeds, the number of outer integument cells at 6 DAP was comparable with that at 8 DAP (Figure 6F), indicating that cells in the outer integuments of wild-type seeds completely stop dividing by 6 DAP. Similarly, cells in the outer integuments of *sod7-2 dpa4-3* seeds also cease division by 6 DAP. The number of outer integument cells in *sod7-2 dpa4-3* seeds was significantly increased compared with that in wild-type seeds (Figure 6F). By contrast, the length of outer integument cells in *sod7-2 dpa4-3* seeds was not increased in comparison to that in wild-type seeds (Figure 6G). We further counted cells in the outer integuments of *sod7-1D* ovules and developing seeds. As shown in Supplemental Figure 8, the outer integuments of *sod7-1D* contained fewer cells than those of the wild type. Thus, *SOD7* and *DPA4* influence cell proliferation in the maternal integuments of ovules and developing seeds.

SOD7 and *DPA4* Act Maternally to Affect Embryo and Endosperm Growth

The reciprocal experiments showed that the embryo and endosperm genotypes for *SOD7* and *DPA4* do not determine seed

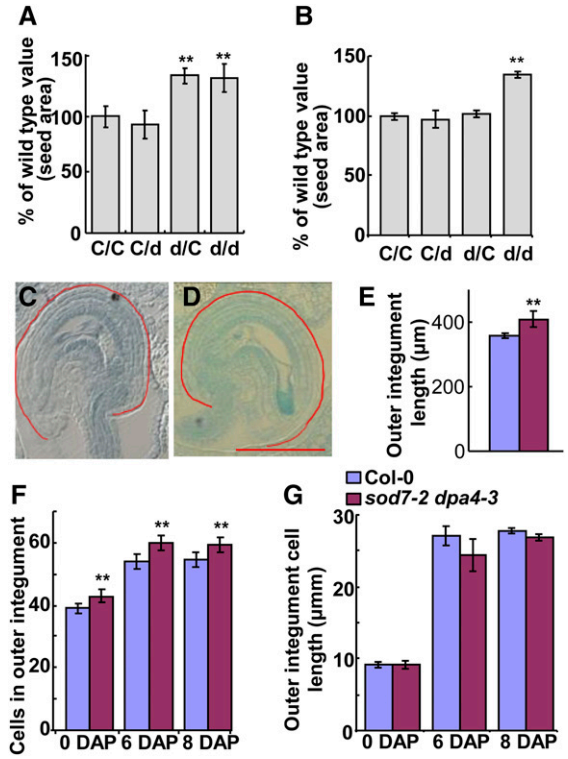

Figure 6. *SOD7* and *DPA4* Act Maternally to Determine Seed Size.

(A) Area of Col-0×Col-0 (C/C) F1, Col-0×*sod7-2 dpa4-3* (C/d) F1, *sod7-2 dpa4-3*×Col-0 (d/C) F1, and *sod7-2 dpa4-3*×*sod7-2 dpa4-3* (d/d) F1 seeds. Values are given as mean ± SD relative to the respective wild-type values, set at 100% (n = 120).

(B) Area of Col-0×Col-0 (C/C) F2, Col-0×*sod7-2 dpa4-3* (C/d) F2, *sod7-2 dpa4-3*×Col-0 (d/C) F2, and *sod7-2 dpa4-3*×*sod7-2 dpa4-3* (d/d) F2 seeds. Values are given as mean ± SD relative to the respective wild-type values, set at 100% (n = 120).

(C) and **(D)** Mature ovules of Col-0 **(C)** and *sod7-2 dpa4-3* **(D)** (n = 60).

(E) Outer integument length of mature Col-0 and *sod7-2 dpa4-3* ovules. Values are given as mean ± SD (n = 60).

(F) The number of cells in the outer integuments of Col-0 and *sod7-2 dpa4-3* at 0, 6, and 8 DAP. Values are given as mean ± SD (n = 30).

(G) The length of cells in the outer integuments of Col-0 and *sod7-2 dpa4-3* at 0, 6, and 8 DAP. Values are given as mean ± SD (n = 100).

P < 0.01 compared with the wild type (Col-0) (Student's t test). Bars = 50 μm in **(C) and **(D)**.

size, and *SOD7* and *DPA4* are required in the sporophytic tissue of the mother plant to regulate seed growth (Figure 6). The *sod7-2 dpa4-3* had larger seed coats than the wild type. The maternal integument or seed coat has been known to act as a physical constraint on embryo and endosperm growth and maternally affect endosperm and embryo development (Jofuku et al., 2005; Ohto et al., 2005, 2009; Adamski et al., 2009; Fang et al., 2012; Xia et al., 2013; Du et al., 2014). Consistent with this, mature *sod7-2 dpa4-3* embryos were significantly larger than wild-type embryos (Figure 5D). The cotyledon area of mature *sod7-2 dpa4-3* embryos was ~163% that of wild-type embryos (Supplemental Figure 9A). Embryo size is determined by both cell number and cell size. We measured palisade cells in wild-type and *sod7-2 dpa4-3* cotyledons to determine which parameter is affected. As shown in Supplemental Figures 9B and 9C, cells in *sod7-2 dpa4-3* cotyledons were slightly larger than those in wild-type cotyledons. The number of cells in *sod7-2 dpa4-3* cotyledons was significantly higher than that in wild-type cotyledons. Thus, these results suggest that *SOD7* acts maternally to influence embryo cell proliferation and cell expansion.

We then asked whether *sod7-2 dpa4-3* integuments could influence embryo development. To test this, we manually pollinated wild-type and *sod7-2 dpa4-3* plants with their own pollen grains and examined developing embryos at specific times after pollination. In the siliques of wild-type plants, most embryos reached the globular stage at 2 DAP, the heart stage at 4 DAP, the torpedo stage at 6 DAP, the bent cotyledon and green embryo stages at 8 DAP, and the stage of the fully filled seed cavity at 11 DAP (Figure 7A). Morphological development of *sod7-2 dpa4-3* embryos was delayed, compared with that of wild-type embryos (Figure 7A). We further investigated whether *sod7-2 dpa4-3* integuments could affect endosperm development. As shown in Figure 7B, the endosperm cellularization in *sod7-2 dpa4-3* seeds was also delayed, compared with that in wild-type seeds. Taken together, these results indicate that *SOD7* acts maternally to influence embryo and endosperm development because *SOD7* is solely required in the sporophytic tissue of the mother plant to control seed growth (Figure 6). It is possible that *sod7-2 dpa4-3* forms a large seed cavity, which provides more space for embryo and endosperm growth and development. This phenomenon of embryo and endosperm development has also been observed in other Arabidopsis large seed mutants that act maternally to regulate seed size (Schruff et al., 2006; Ohto et al., 2009; Fang et al., 2012).

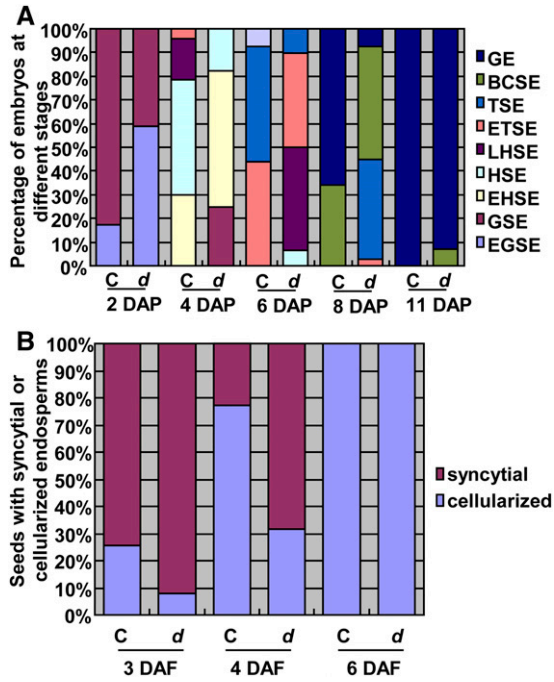

Figure 7. *SOD7* and *DPA4* Act Maternally to Influence Embryo and Endosperm Development.

(A) Percentage of embryos at different stages was recorded for Col-0 **(C)** and *sod7-ko1 ngal3-ko1* **(D)**, and at least 80 seeds were investigated for each genotype. EGSE, early globular stage embryo; GSE, globular stage embryo; EHSE, early heart stage embryo; HSE, heart stage embryo; LHSE, late heart stage embryo; ETSE, early torpedo stage embryo; TSE, torpedo stage embryo; BCSE, bent cotyledon stage embryo; GE, green stage embryo.

(B) Percentage of Col-0 **(C)** and *sod7-ko1 ngal3-ko1* **(D)** seeds with syncytial or cellularized endosperms was recorded. EM, embryo; CE, cellularized endosperm; DAF, day after fertilization.

SOD7 and *DPA4* Act in a Common Pathway with *KLU* to Regulate Seed Size, but Do So Independently of *DA1*

The Arabidopsis *klu* mutants formed small seeds due to the decreased cell proliferation in the integuments, while plants overexpressing *KLU*/*CYP78A5* produced large seeds as a result of the increased cell proliferation in the integuments (Adamski et al., 2009), suggesting that *SOD7* and *KLU* function antagonistically in a common pathway to regulate seed growth. To test for genetic interactions between *SOD7* and *KLU*, we generated the *klu-4 sod7-2 dpa4-3* triple mutant and measured the size of seeds from wild-type, *klu-4*, *sod7-2 dpa4-3*, and *klu-4 sod7-2 dpa4-3* plants. As shown in Figures 8A and 8B, the average size and weight of *klu-4 sod7-2 dpa4-3* seeds were similar to those of the *klu-4* single mutant, indicating that *klu-4* is epistatic to *sod7-2 dpa4-3* with respect to seed size and weight. We further investigated the mature ovules from wild-type, *klu-4*, *sod7-2 dpa4-3*, and *klu-4 sod7-2 dpa4-3* plants. The outer integument length of *klu-4 sod7-2 dpa4-3* ovules was comparable with that of *klu-4* ovules (Figure 8C). Similarly, the outer integument length of *klu-4 sod7-2 dpa4-3* seeds was indistinguishable from that of *klu-4* seeds at 8 DAP (Figure 8C). In addition, the size of *klu-4 sod7-2 dpa4-3* petals was more similar to that of *klu-4* petals than to that of *sod7-2 dpa4-3* petals (Supplemental Figure 10A). Expression patterns of *SOD7* and *KLU* in young petals partially overlapped (Supplemental Figure 10B). Thus, *klu-4* is epistatic to *sod7-2 dpa4-3* with respect to seed and organ size, indicating that *SOD7* and *DPA4* act in a common pathway with *KLU* to regulate seed and organ growth.

To further understand the cellular basis of epistatic interactions between *SOD7* and *KLU*, we investigated the outer integument cell number of ovules and developing seeds from wild-type, *klu-4*, *sod7-2 dpa4-3*, and *klu-4 sod7-2 dpa4-3* plants. The number of outer integument cells in *klu-4 sod7-2 dpa4-3* ovules was similar to that in *klu-4* ovules (Figure 8D). Similarly, the number of outer integument cells in *klu-4 sod7-2 dpa4-3* seeds was comparable with

that in *klu-4* seeds (Figure 8D). These results indicate that *klu-4* is epistatic to *sod7-2 dpa4-3* with respect to the number of outer integument cells. We also observed that cells in the outer integuments of *klu-4* and *klu-4 sod7-2 dpa4-3* seeds were slightly longer than those in wild-type seeds (Supplemental Figure 11), suggesting the existence of a possible compensation mechanism between cell proliferation and cell expansion. Together, these findings show that *SOD7* and *DPA4* function antagonistically in a common pathway with *KLU* to regulate cell proliferation in the maternal integuments.

Considering that *sod7-1D* was identified as a suppressor of *da1-1* in seed size, we further asked whether *SOD7* and *DA1* could act in the same genetic pathway. To test this, we measured the size of wild-type, *da1-1*, *sod7-1D*, and *sod7-1D da1-1* seeds. The genetic interaction between *sod7-1D* and *da1-1* was essentially additive for seed size, compared with that of *sod7-1D* and *da1-1* single mutants (Supplemental Figure 12A), indicating that *SOD7* might function independently of *DA1* to regulate seed size. We further crossed *sod7-2 dpa4-3* with *da1-1* and generated the *sod7-2 dpa4-3 da1-1* triple mutant and measured its seed size. The genetic interaction between *sod7-2 dpa4-3* and *da1-1* was also additive for seed size, compared with their parental lines (Supplemental Figure 12B), further supporting the notion that *SOD7* and *DPA4* regulate seed growth separately from *DA1*.

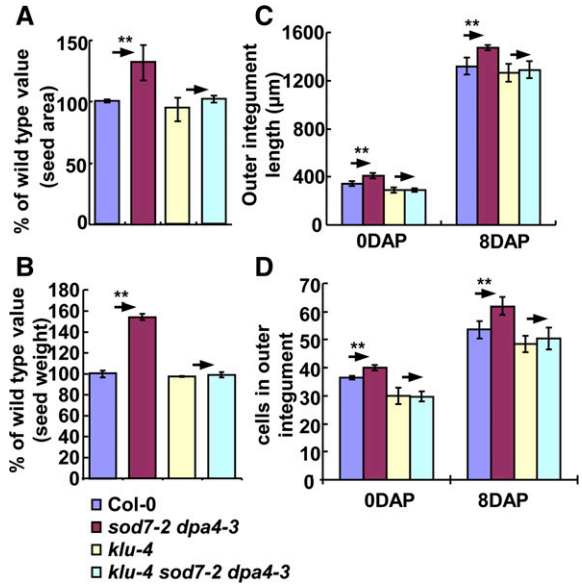

Figure 8. *klu-4* Is Epistatic to *sod7-2 dpa4-3* with Respect to Seed Size.

(A) Seed area of Col-0, *klu-4*, *sod7-2 dpa4-3*, and *klu-4 sod7-2 dpa4-3.* Values are given as mean ± SD relative to the respective wild-type values, set at 100% (n = 120).

(B) Seed weight of Col-0, *klu-4*, *sod7-2 dpa4-3*, and *klu-4 sod7-2 dpa4-3.* Values are given as mean ± SD relative to the respective wild-type values, set at 100%. The weights of five sample batches were measured for each seed lot (n = 5).

(C) The outer integument length of Col-0, *klu-4*, *sod7-2 dpa4-3*, and *klu-4 sod7-2 dpa4-3* at 0 and 8 DAP. Values are given as mean ± SD (n = 60).

(D) The number of cells in the outer integuments of Col-0, *klu-4*, *sod7-2 dpa4-3*, and *klu-4 sod7-2 dpa4-3* at 0 and 8 DAP. Values are given as mean ± SD (n = 30).

**P < 0.01 compared with their respective controls (Student's t test).

SOD7 Directly Binds to the Promoter of *KLU* and Represses the Expression of *KLU*

Considering that *SOD7* acts antagonistically in a common pathway with *KLU* to regulate seed size, we asked whether the transcription repressor SOD7 could repress the expression of *KLU*. We therefore investigated the expression of *KLU* in the chemically-inducible *SOD7* (*pER8-SOD7*) transgenic plants. After the *pER8-SOD7* transgenic plants were treated with the inducer (β-estradiol), the expression of *SOD7* was induced at 4 and 8 h (Figure 9A). As expected, the expression of *KLU* was significantly repressed at 4 and 8 h (Figure 9A). We further detected the expression of *KLU* in wild-type and *sod7-2 dpa4-3* ovules using in situ hybridization. As shown in Figure 9B, the expression of *KLU* in the inner integuments of *sod7-2 dpa4-3* ovules was markedly increased, compared with that in the inner integuments of wild-type ovules. Thus, these results indicate that *SOD7* represses the expression of *KLU* and also suggest that *KLU* is a direct target of *SOD7*.

To determine whether SOD7 can directly bind to the promoter of *KLU*, we performed a chromatin immunoprecipitation (ChIP) assay with *Pro35S:GFP* and *Pro35:GFP-SOD7* transgenic plants. It has been reported that the CACCTG sequence is recognized by the B3 domain of RAV1, one member of the RAV family (Kagaya et al., 1999; Yamasaki et al., 2004). We therefore analyzed the 2-kb promoter sequence of *KLU*, but did not find an intact CACCTG sequence. However, we found a similar sequence (CACTTG) in the promoter region of *KLU* (Figure 9B), which could be the potential SOD7 binding site. To test this, we examined the enrichment of a *KLU* promoter fragment (PF1) containing the CACTTG sequence by ChIP analysis and found that PF1 was strongly enriched in the chromatin-immunoprecipitated DNA with anti-GFP antibody (Figures 9C and 9D). By contrast, we did not detect significant enrichment of an *ACTIN7* promoter sequence and the *KLU* promoter fragment PF2, which does not contain the CACTTG sequence (Figures 9C and 9D). Therefore, SOD7 associates with the *KLU* promoter in vivo. We further expressed SOD7 as a MBP fusion protein (MBP-SOD7) and performed a DNA electrophoretic mobility shift assay (EMSA). As shown in Figures 9C and 9E, MBP-SOD7 bound to biotin-labeled probe *A* containing the CACTTG sequence, and the binding was reduced by the addition of an unlabeled probe *A*. By contrast, MBP-SOD7 failed to bind to a probe *A-m* with mutations in the CACTTG sequence (Figures 9C and 9E). Taken together, these results show that SOD7 directly binds to the promoter of *KLU* and represses *KLU* expression.

DISCUSSION

Seed size is crucial for plant fitness and agricultural purposes. Several factors that act maternally to influence seed size have been described in Arabidopsis, such as TTG2, AP2, ARF2, KLU, DA1, DA2, and SOD2/UBP15. DA1 acts synergistically with E3 ubiquitin ligases DA2 and EOD1 to restrict seed and organ growth (Xia et al., 2013). DA1 interacts with SOD2 and modulates the stability of SOD2 to regulate seed and organ size (Du et al., 2014). In this study, we identify another *SOD7*, which acts maternally to regulate seed size by restricting cell proliferation in the integuments of ovules and developing seeds. *SOD7* encodes a B3 domain transcriptional repressor NGAL2 and acts redundantly with its

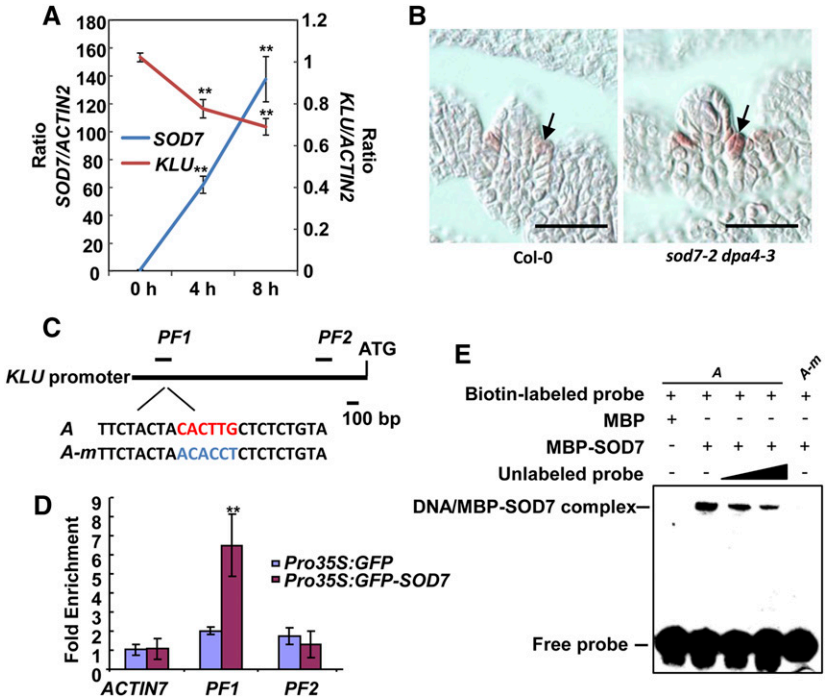

Figure 9. SOD7 Directly Binds to the Promoter of *KLU* and Represses the Expression of *KLU*.

(A) Expression dynamics of *SOD7* and *KLU* in *pER8-SOD7* transgenic plants treated with β-estradiol for 0, 4, and 8 h. Means were calculated from three biological samples. Values are given as mean ± SD. **P < 0.01, compared with the expression level of *KLU* and *SOD7* at 0 h (Student's *t* test).
(B) Results of in situ hybridization with *KLU* antisense probe. The arrows indicate the inner integument cells in Col-0 and *sod7-2 dpa4-3* ovules. Three independent experiments show similar results. Bars = 100 μm.
(C) A 2-kb promoter region of *KLU* upstream of its ATG codon contains a CACTTG sequence. *PF1* and *PF2* represent PCR fragments used for ChIP-quantitative PCR analysis. *A* and *A-m* indicate the wild-type probe and the mutated probe used in the EMSA, respectively.
(D) ChIP-quantitative PCR analysis shows that SOD7 binds to the promoter fragment PF1 of *KLU*. Chromatin from *Pro35S:GFP* and *Pro35S:GFP-SOD7* transgenic plants was immunoprecipitated by anti-GFP, and the enrichment of the fragments was determined by quantitative real-time PCR. The *ACTIN7* promoter was used as a negative control. The fold enrichment was normalized to the *ACTIN7* amplicon, set at 1. Means were calculated from three biological samples. Values are given as mean ± SD. **P < 0.01, compared with *Pro35S:GFP* transgenic plants (Student's *t* test).
(E) Direct interaction between SOD7 and the *KLU* promoter determined by EMSA. The biotin-labeled probe *A* and MBP-SOD7 formed a DNA-protein complex, but the mutated probe *A-m* and MBP-SOD7 did not. The retarded DNA-protein complex was reduced by competition using unlabeled probe *A*.

closest homolog *NGAL3*/*DPA4* to regulate seed size. Genetic analyses indicate that SOD7 and DPA4 function in a common pathway with the maternal factor KLU to regulate seed growth, but do so independently of DA1. Further results reveal that SOD7 directly binds to the promoter region of *KLU* and represses *KLU* expression. Thus, our findings identify SOD7 and DPA4 as negative factors for seed size and define the genetic and molecular mechanisms of SOD7, DPA4, and KLU in seed size control.

SOD7 and *DPA4* Act Maternally to Regulate Seed Size

The *sod7-1D* gain-of-function mutant was identified as a suppressor of the large seed phenotype of *da1-1*. However, genetic analyses showed that *SOD7* functions independently of *DA1* to regulate seed growth (Supplemental Figure 12). The *sod7-1D* single mutant produced small seeds and organs (Figure 2), while the simultaneous disruption of *SOD7* and the closely related family member *DPA4*/*NGAL3* resulted in large seeds and organs (Figure 5), indicating that SOD7 is a negative regulator of seed and organ size. Several previous studies suggest that there is a possible link between seed size and organ growth. For instance, *arf2*, *da1-1*, *da2-1*, and *eod3-1D* mutants produced large seeds and organs (Schruff et al., 2006; Li et al., 2008; Fang et al., 2012; Xia et al., 2013), whereas *klu* and *sod2*/*ubp15* mutants formed small seeds and organs (Anastasiou et al., 2007; Adamski et al., 2009; Du et al., 2014). However, seed size is not invariably associated with organ size. For example, *eod8*/*med25* mutants with large organs formed normal-sized seeds (Xu and Li, 2011), while *ap2* mutants with normal-sized organs produced large seeds (Jofuku et al., 2005; Ohto et al., 2005). Thus, these findings suggest that seeds and organs not only possess distinct pathways but also share common mechanisms to regulate their size. In this study, our results show that *SOD7* and *DPA4* redundantly restrict both seed and organ growth in Arabidopsis.

Reciprocal cross experiments showed that *SOD7* and *DPA4* act maternally to restrict seed growth, and the endosperm and embryo genotypes for *SOD7* and *DPA4* do not determine seed size (Figure 6). The integuments surrounding the ovule are

maternal tissues and form the seed coat after fertilization. Arabidopsis *arf2*, *ap2*, *da1-1*, *da2-1*, and *eod3-1D* mutants with large integuments formed large seeds (Jofuku et al., 2005; Ohto et al., 2005; Schruff et al., 2006; Li et al., 2008; Fang et al., 2012; Xia et al., 2013), while *klu-4* and *ubp15/sod2* mutants with small integuments produced small seeds (Adamski et al., 2009; Du et al., 2014), indicating that the maternal integuments are crucial for determining seed size in Arabidopsis. Consistent with this notion, mature *sod7-2 dpa4-3* ovules were larger than wild-type ovules (Figures 6C and 6D). The outer integument length of *sod7-2 dpa4-3* ovules and developing seeds was significantly increased compared with that of wild-type ovules and seeds (Figures 6E and 7C). Thus, the regulation of maternal integument size is an important mechanism for seed size control. The maternal integument acts as a physical constraint on embryo and endosperm growth and influences endosperm and embryo development (Jofuku et al., 2005; Ohto et al., 2005, 2009; Adamski et al., 2009; Fang et al., 2012; Xia et al., 2013; Du et al., 2014). Consistent with this, embryo and endosperm development in *sod7-2 dpa4-3* was delayed, compared with that in the wild type (Figures 7A and 7B). Thus, it is plausible that *sod7-2 dpa4-3* has a large seed cavity, which provides more space for embryo and endosperm growth and affects embryo and endosperm development. In support of this notion, large seed mutants that act maternally to influence seed size usually exhibited a prolonged period of seed growth and delayed embryo and endosperm development in Arabidopsis (Schruff et al., 2006; Ohto et al., 2009; Fang et al., 2012).

The size of the integument is determined by cell proliferation and cell expansion; these two processes are assumed to be coordinated. The number of outer integument cells in *sod7-2 dpa4-3* ovules and seeds was significantly increased compared with that in wild-type ovules and seeds (Figure 6F), indicating that *SOD7* and *DPA4* regulate seed growth by limiting cell proliferation in the maternal integuments. Similarly, several mutants with the increased number of cells in the maternal integuments produced large seeds in Arabidopsis (Schruff et al., 2006; Li et al., 2008; Xia et al., 2013). By contrast, several other mutants with a decreased number of cells in the maternal integuments formed small seeds in Arabidopsis (Adamski et al., 2009; Du et al., 2014). Considering that cells in the integuments mainly undergo expansion after fertilization (Garcia et al., 2005), it is possible that the number of cells in the integuments determines the growth potential of the seed coat after fertilization.

The Genetic and Molecular Mechanisms of *SOD7* and *KLU* in Seed Size Regulation

The *sod7-1D* mutant had small seeds and organs (Figure 2), as had been seen in *klu* mutants (Anastasiou et al., 2007; Adamski et al., 2009). *KLU* encodes a cytochrome P450 CYP78A5 that has been proposed to generate mobile plant growth substances (Anastasiou et al., 2007; Adamski et al., 2009). *KLU* regulates seed size by promoting cell proliferation in the maternal integuments of ovules (Anastasiou et al., 2007; Adamski et al., 2009). By contrast, *SOD7* acts maternally to control seed size by limiting cell proliferation in the integuments of ovules and developing seeds (Figure 6). These results suggest that *SOD7* could function antagonistically in a common pathway with *KLU* to regulate seed size. In our growth conditions, *klu-4* formed slightly smaller seeds than the wild type due to the decreased cell number and the slightly increased cell length in the integuments of developing seeds (Figures 8A and 8D; Supplemental Figure 11), suggesting a possible compensation mechanism between cell proliferation and cell expansion in *klu-4* integuments. Importantly, our genetic analyses showed that *klu-4* is epistatic to *sod7-2 dpa4-3* with respect to seed and organ size (Figures 8A and 8B; Supplemental Figure 10A). *klu-4* is also epistatic to *sod7-2 dpa4-3* for the outer integument length (Figure 8C). Further results revealed that the number of cells in the outer integuments of *klu-4 sod7-2 dpa4-3* ovules and developing seeds was similar to that of *klu-4* ovules and developing seeds (Figure 8D). Thus, these genetic results demonstrate that *SOD7* and *DPA4* act in a common pathway with *KLU* to modulate seed size by regulating cell proliferation in the maternal integuments.

SOD7 encodes a B3 domain transcriptional repressor NGAL2 that is localized in nuclei of Arabidopsis cells (Figures 4P to 4S; Supplemental Figures 4D to 4I). Thus, it is possible that SOD7 directly binds to the promoter of *KLU* and represses *KLU* expression. *SOD7* and *KLU* have overlapping expression patterns during ovule and seed development. For example, *SOD7* and *KLU* expression was stronger in younger ovules than in older ones (Figures 4L to 4O) (Adamski et al., 2009). After fertilization, the expression of both *SOD7* and *KLU* was hardly detected (Supplemental Figure 13). Importantly, the inducible expression of *SOD7* resulted in a significantly reduction of *KLU* expression (Figure 9A). Our ChIP-quantitative PCR data showed that SOD7 associates with the promoter region of *KLU* in vivo (Figures 9B and 9C). EMSA experiments revealed that SOD7 directly binds to the CACTTG sequence in the promoter of *KLU* (Figures 9B and 9D). Thus, these results illustrate that SOD7 directly targets the promoter region of *KLU* and represses the expression of *KLU*, thereby determining seed size. Interestingly, the gain-of-function mutant *sod7-1D* had smaller seeds than *klu-4*, suggesting that overexpression of *SOD7* might also repress the expression of other target genes. Taken together, these findings reveal the genetic and molecular mechanisms of *SOD7*, *DPA4*, and *KLU* in regulating Arabidopsis seed size.

For many plants, the seeds are the main product to be harvested, and an increase in seed size would be beneficial for growers. In this study, we identify SOD7 and DPA4 as negative regulators of seed size and demonstrate that *SOD7* and *DPA4* act in a common genetic pathway with *KLU* to regulate seed size. Our current knowledge of *SOD7* functions suggests that *SOD7* (and its homologs in other plant species) could be used to engineer large seed size in crops. Considering that crop plants have undergone selection for large seed size during domestication (Fan et al., 2006; Song et al., 2007; Gegas et al., 2010), it will be worthwhile establishing whether beneficial alleles of *SOD7* homologs have already been utilized by plant breeders.

METHODS

Plant Materials and Growth Conditions

Arabidopsis thaliana Col-0 was used as the wild-type line. The *da1-1*, *sod7-1D*, *sod7-2*, and *dpa4-3* were in the Col-0 background. *sod7-1D* was identified as a suppressor of *da1-1* using a T-DNA activation-tagging method. *sod7-2* (SM_3.34191) and *dpa4-3* (SM_3.36641) were identified in SIGnAL (http://signal.salk.edu/cgi-bin/tdnaexpress/) and obtained from the Arabidopsis stock center NASC collection. dSpm transposon

insertions were confirmed by PCR and sequencing using the primers described in Supplemental Table 1. Arabidopsis plants were grown under long-day conditions (16 h light/8 h dark) at 22°C.

Activation-Tagging Screening

The activation-tagging plasmid *pJFAT260* was introduced into the *da1-1* mutant plants using *Agrobacterium tumefaciens* strain GV3101 (Fan et al., 2009; Fang et al., 2012), and T1 plants were selected using the herbicide Basta. Seeds produced from T1 plants were used to isolate modifiers of *da1-1*.

Morphological and Cellular Analysis

To measure seed size, we photographed dry seeds of the wild type and mutants under a Leica microscope (Leica S8APO) using Leica CCD (DFC420). The area of wild-type and mutant seeds was measured using ImageJ software. Average seed weight was determined by weighing mature dry seeds in batches of 100 using an electronic analytical balance (Mettler Toledo AL104). The weights of five sample batches were measured for each seed lot.

Fully expanded cotyledons, petals (stage 14), and leaves were scanned to produce digital images for area measurement. To measure cell number and cell size, petals, leaves, ovules, and seeds were placed in a drop of clearing solution (30 mL water, 80 g chloral hydrate [Sigma-Aldrich C8383], and 10 mL 100% glycerol [Sigma-Aldrich G6279]). Cleared samples were imaged under a Leica microscope (Leica DM2500) with differential interference contrast optics and photographed with a Spot Flex cooled CCD digital imaging system. Area measurement was made using ImageJ software.

Cloning of *SOD7*

The flanking sequences of the T-DNA insertion of the *sod7-1D* mutant were identified by TAIL-PCR according to a previously reported method (Liu et al., 1995). Briefly, TAIL-PCR uses three nested specific primers (OJF22, OJF23, and OJF24) within the T-DNA region of the *pJFAT260* vector and a shorter arbitrary degenerate primer (AD1). Thus, the relative amplification efficiencies of specific and nonspecific products can be thermally controlled. TAIL-PCR products were sequenced using the primer OJF24. The specific primers OJF22, OJF23, and OJF24 and an arbitrary degenerate (AD1) primer are described in Supplemental Table 1.

Constructs and Plant Transformation

The *35S:GFP-SOD7*, *ProSOD7:SOD7-GFP*, and *ProSOD7:GUS* constructs were made using a PCR-based Gateway system. The coding sequence (CDS) of *SOD7* was amplified using the primers SOD7CDS-F and SOD7CDS-R (Supplemental Table 1). PCR products were cloned into the *pCR8/TOPO TA* cloning vector. The *SOD7* CDS was then subcloned into the binary vector *pMDC43* with the *GFP* gene to generate the transformation plasmid *Pro35S:GFP-SOD7.* The *SOD7* genomic sequence containing a 2040-bp promoter sequence and 2104-bp *SOD7* gene was amplified using the primers SOD7G-F and SOD7G-R (Supplemental Table 1). PCR products were cloned into the *pCR8/TOPO TA* cloning vector. The *SOD7* genomic sequence was then subcloned into the binary vector *pMDC107* with the *GFP* gene to generate the transformation plasmid *pSOD7:SOD7-GFP*. The 2262-bp *SOD7* promoter sequence was amplified using the primers SOD7P-F and SOD7P-R (Supplemental Table 1). PCR products were cloned into the *pCR8/TOPO TA* cloning vector. The *SOD7* promoter was then subcloned into the binary vector *pGWB3* with the *GUS* gene to generate the transformation plasmid *pSOD7:GUS*. The plasmids *35S:GFP-SOD7*, *pSOD7:SOD7-GFP*, and *pSOD7:GUS* were introduced into Col-0 and *sod7-2 dpa4-3* plants using Agrobacterium GV3101, respectively, and transformants were selected on medium containing 30 μg/mL hygromycin.

The *SOD7* cDNA was cloned into the *Apa*I and *Spe*I sites of the binary vector *pER8* to generate a chemically inducible construct *pER8-SOD7*. The specific primers for the *pER8-SOD7* construct were SOD7ER-F and SOD7ER-R. The plasmid *pER8-SOD7* was introduced into Col-0 plants using Agrobacterium GV3101, and transformants were selected on medium containing 30 μg/mL hygromycin.

GUS Staining

Samples (*ProSOD7:GUS*) were stained in a GUS staining solution [1 mM X-Gluc, 50 mM $NaPO_4$ buffer, 0.4 mM each $K_3Fe(CN)6/K_4Fe(CN)_6$, and 0.1% (v/v) Triton X-100] and incubated at 37°C for 3 h. After GUS staining, chlorophyll was removed by washing with 70% ethanol.

RT-PCR and Quantitative Real-Time RT-PCR

Total RNA was extracted from Arabidopsis seedlings using an RNAprep pure Plant Kit (Tiangen). mRNA was reverse transcribed into cDNA using SuperScriptIII reverse transcriptase (Invitrogen). cDNA samples were standardized on *ACTIN2* transcript amount using the primers ACTIN2-F and ACTIN2-R (Supplemental Table 1). Quantitative real-time RT-PCR analysis was performed with a Lightcycler 480 machine (Roche) using the Lightcycler 480 SYBR Green I Master (Roche). *ACTIN2* mRNA was used as an internal control, and relative amounts of mRNA were calculated using the comparative threshold cycle method. The primers used for RT-PCR and quantitative real-time RT-PCR are described in Supplemental Table 1.

RNA in Situ Hybridization

In situ hybridization was performed as described (Li et al., 2003; Fang et al., 2012). DIG-labeled RNA transcripts were generated by transcription of *KLU* in antisense orientation using T7 RNA polymerase (Roche). After hybridization, washing, and blocking, DIG-labeled RNA transcripts reacting with alkaline phosphatase-conjugated anti-DIG Fab fragment (1:3000 [v/v]; Roche) were detected using 5-bromo-4-chloro-3-indolyl phosphate/nitroblue tetrazolium. The slides were observed with a microscope (Leica DM2500) and photographed using a Spot Flex cooled CCD digital imaging system.

The ChIP Assay

The ChIP assay was performed as described previously with minor modifications (Gendrel et al., 2005). Briefly, *Pro35S:GFP* and *Pro35S:GFP-SOD7* transgenic seeds were grown on half-strength Murashige and Skoog plates for 10 d. The seedlings were cross-linked with 1% formaldehyde for 15 min in vacuum and stopped by 0.125 M glycine. Samples were ground in liquid nitrogen, and nuclei were isolated. Chromatin was immunoprecipitated by anti-GFP (Roche; 11814460001) and protein A+G beads (Millipore Magna ChIP Protein A+G magnetic beads). DNA was precipitated with glycogen, NaOAc, and ethanol, washed with 70% ethanol, and dissolved in 60 μL of water. Gene-specific primers (PF1-F, PF1-R, PF2-F, PF2-R, ACTIN7-ChIP-F, and ACTIN7-ChIP-R) were used to quantify the enrichment of each fragment (Supplemental Table 1).

DNA EMSA

The coding sequence of *SOD7* was cloned into the *Nde*I and *Bam*HI sites of the *pMAL-C2* vector to generate the *MBP-SOD7* construct. MBP-SOD7 fusion proteins were expressed in *Escherichia coli* BL21 (DE3) (Biomed) and purified on Amylose resin (New England Biolabs). The biotin-labeled and unlabeled probes were synthesized as forward and reverse strands. The forward and reverse strands were then incubated in a solution (50 mM Tris-HCl, 5 mM EDTA, and 250 mM NaCl) at 95°C for 10 min and renatured to double stranded probes at room temperature.

The gel shift assay was performed according to a method described previously (Smaczniak et al., 2012).

Accession Numbers

Arabidopsis Genome Initiative locus identifiers for genes mentioned in this article are as follows: At1g19270 (*DA1*), At1g13710 (KLU), At3g11580 (*SOD7*/*NGAL2*), and At5g06250 (*DPA4*/*NGAL3*).

Supplemental Data

Supplemental Figure 1. The organ size phenotype of the *sod7-1D* mutant.

Supplemental Figure 2. The organ size phenotype of *Pro35S:GFP-SOD7* transgenic plants.

Supplemental Figure 3. Phylogenetic tree of the RAV family members in Arabidopsis.

Supplemental Figure 4. Subcellular localization of *SOD7.*

Supplemental Figure 5. Identification of *sod7-2* and *dpa4-3* mutants.

Supplemental Figure 6. *SOD7* acts redundantly with *DPA4* to influence organ size.

Supplemental Figure 7. *SOD7* does not affect flowering time.

Supplemental Figure 8. The number of cells in the outer integuments of Col-0 and *sod7-1D.*

Supplemental Figure 9. Cell size and cell number in cotyledons of mature wild-type and *sod7-2 dpa4-3* embryos.

Supplemental Figure 10. *klu-4* is epistatic to *sod7-2 dpa4-3* with respect to organ size.

Supplemental Figure 11. Outer integument cell length of Col-0, *klu-4*, *sod7-2 dpa4-3*, and *klu-4 sod7-2 dpa4-3* seeds.

Supplemental Figure 12. *SOD7* acts independently of *DA1* to regulate seed size.

Supplemental Figure 13 . Expression of *SOD7* and *KLU* in developing seeds.

Supplemental Table 1. Primers used in this study.

Supplemental Data Set 1. Alignments used to generate the phylogeny presented in Supplemental Figure 3.

ACKNOWLEDGMENTS

We thank the anonymous reviewers and the editor for their helpful comments on this article, Jun Fan for the *pJFAT260* vector, Michael Lenhard for the *klu-4* mutant (SM_3.39145), Nam-Hai Chua for the *pER8* vector, and the Arabidopsis stock centers ABRC and NASC for *sod7-2* and *dpa4-3* mutants. This work was supported by grants from the National Natural Science Foundation of China (91417304, 31425004, 91017014, 31221063, and 31100865) and the National Basic Research Program of China (2009CB941503).

AUTHOR CONTRIBUTIONS

Y.Z. and Y.L. designed the research. Y.Z. performed most of the experiments. L.D. and R.X. identified the *SOD7* gene. R.C. performed the in situ hybridization experiment. J.H. and C.S. conducted the TAIL-PCR assay. Y.Z. and Y.L. analyzed the data. Y.L. wrote the article.

Received December 13, 2014; revised February 10, 2015; accepted February 26, 2015; published March 17, 2015.

REFERENCES

Adamski, N.M., Anastasiou, E., Eriksson, S., O'Neill, C.M., and Lenhard, M. (2009). Local maternal control of seed size by KLUH/CYP78A5-dependent growth signaling. Proc. Natl. Acad. Sci. USA **106:** 20115–20120.

Alvarez, J.P., Goldshmidt, A., Efroni, I., Bowman, J.L., and Eshed, Y. (2009). The NGATHA distal organ development genes are essential for style specification in Arabidopsis. Plant Cell **21:** 1373–1393.

Anastasiou, E., Kenz, S., Gerstung, M., MacLean, D., Timmer, J., Fleck, C., and Lenhard, M. (2007). Control of plant organ size by KLUH/CYP78A5-dependent intercellular signaling. Dev. Cell **13:** 843–856.

Cheng, Z.J., Zhao, X.Y., Shao, X.X., Wang, F., Zhou, C., Liu, Y.G., Zhang, Y., and Zhang, X.S. (2014). Abscisic acid regulates early seed development in Arabidopsis by ABI5-mediated transcription of SHORT HYPOCOTYL UNDER BLUE1. Plant Cell **26:** 1053–1068.

Du, L., Li, N., Chen, L., Xu, Y., Li, Y., Zhang, Y., Li, C., and Li, Y. (2014). The ubiquitin receptor DA1 regulates seed and organ size by modulating the stability of the ubiquitin-specific protease UBP15/SOD2 in Arabidopsis. Plant Cell **26:** 665–677.

Engelhorn, J., Reimer, J.J., Leuz, I., Göbel, U., Huettel, B., Farrona, S., and Turck, F. (2012). Development-related PcG target in the apex 4 controls leaf margin architecture in *Arabidopsis thaliana*. Development **139:** 2566–2575.

Fan, C., Xing, Y., Mao, H., Lu, T., Han, B., Xu, C., Li, X., and Zhang, Q. (2006). GS3, a major QTL for grain length and weight and minor QTL for grain width and thickness in rice, encodes a putative transmembrane protein. Theor. Appl. Genet. **112:** 1164–1171.

Fan, J., Hill, L., Crooks, C., Doerner, P., and Lamb, C. (2009). Abscisic acid has a key role in modulating diverse plant-pathogen interactions. Plant Physiol. **150:** 1750–1761.

Fang, W., Wang, Z., Cui, R., Li, J., and Li, Y. (2012). Maternal control of seed size by EOD3/CYP78A6 in *Arabidopsis thaliana*. Plant J. **70:** 929–939.

Garcia, D., Fitz Gerald, J.N., and Berger, F. (2005). Maternal control of integument cell elongation and zygotic control of endosperm growth are coordinated to determine seed size in Arabidopsis. Plant Cell **17:** 52–60.

Garcia, D., Saingery, V., Chambrier, P., Mayer, U., Jürgens, G., and Berger, F. (2003). Arabidopsis haiku mutants reveal new controls of seed size by endosperm. Plant Physiol. **131:** 1661–1670.

Gegas, V.C., Nazari, A., Griffiths, S., Simmonds, J., Fish, L., Orford, S., Sayers, L., Doonan, J.H., and Snape, J.W. (2010). A genetic framework for grain size and shape variation in wheat. Plant Cell **22:** 1046–1056.

Gendrel, A.V., Lippman, Z., Martienssen, R., and Colot, V. (2005). Profiling histone modification patterns in plants using genomic tiling microarrays. Nat. Methods **2:** 213–218.

Harper, J.L., Lovell, P.H., and Moore, K.G. (1970). The shapes and sizes of seeds. Annu. Rev. Ecol. Syst. **1:** 327–356.

Ikeda, M., and Ohme-Takagi, M. (2009). A novel group of transcriptional repressors in Arabidopsis. Plant Cell Physiol. **50:** 970–975.

Jofuku, K.D., Omidyar, P.K., Gee, Z., and Okamuro, J.K. (2005). Control of seed mass and seed yield by the floral homeotic gene APETALA2. Proc. Natl. Acad. Sci. USA **102:** 3117–3122.

Kagaya, Y., Ohmiya, K., and Hattori, T. (1999). RAV1, a novel DNA-binding protein, binds to bipartite recognition sequence through two distinct DNA-binding domains uniquely found in higher plants. Nucleic Acids Res. **27:** 470–478.

Kang, X., Li, W., Zhou, Y., and Ni, M. (2013). A WRKY transcription factor recruits the SYG1-like protein SHB1 to activate gene expression and seed cavity enlargement. PLoS Genet. **9:** e1003347.

Li, J., Nie, X., Tan, J.L., and Berger, F. (2013). Integration of epigenetic and genetic controls of seed size by cytokinin in Arabidopsis. Proc. Natl. Acad. Sci. USA **110:** 15479–15484.

Li, Y., Qian, Q., Zhou, Y., Yan, M., Sun, L., Zhang, M., Fu, Z., Wang, Y., Han, B., Pang, X., Chen, M., and Li, J. (2003). BRITTLE CULM1, which encodes a COBRA-like protein, affects the mechanical properties of rice plants. Plant Cell **15:** 2020–2031.

Li, Y., Zheng, L., Corke, F., Smith, C., and Bevan, M.W. (2008). Control of final seed and organ size by the DA1 gene family in *Arabidopsis thaliana*. Genes Dev. **22:** 1331–1336.

Liu, Y.G., Mitsukawa, N., Oosumi, T., and Whittier, R.F. (1995). Efficient isolation and mapping of Arabidopsis thaliana T-DNA insert junctions by thermal asymmetric interlaced PCR. Plant J. **8:** 457–463.

Lopes, M.A., and Larkins, B.A. (1993). Endosperm origin, development, and function. Plant Cell **5:** 1383–1399.

Luo, M., Dennis, E.S., Berger, F., Peacock, W.J., and Chaudhury, A. (2005). MINISEED3 (MINI3), a WRKY family gene, and HAIKU2 (IKU2), a leucine-rich repeat (LRR) KINASE gene, are regulators of seed size in Arabidopsis. Proc. Natl. Acad. Sci. USA **102:** 17531–17536.

Moles, A.T., Ackerly, D.D., Webb, C.O., Tweddle, J.C., Dickie, J.B., and Westoby, M. (2005). A brief history of seed size. Science **307:** 576–580.

Ohto, M.A., Fischer, R.L., Goldberg, R.B., Nakamura, K., and Harada, J.J. (2005). Control of seed mass by APETALA2. Proc. Natl. Acad. Sci. USA **102:** 3123–3128.

Ohto, M.A., Floyd, S.K., Fischer, R.L., Goldberg, R.B., and Harada, J.J. (2009). Effects of APETALA2 on embryo, endosperm, and seed coat development determine seed size in Arabidopsis. Sex. Plant Reprod. **22:** 277–289.

Orsi, C.H., and Tanksley, S.D. (2009). Natural variation in an ABC transporter gene associated with seed size evolution in tomato species. PLoS Genet. **5:** e1000347.

Schruff, M.C., Spielman, M., Tiwari, S., Adams, S., Fenby, N., and Scott, R.J. (2006). The AUXIN RESPONSE FACTOR 2 gene of Arabidopsis links auxin signalling, cell division, and the size of seeds and other organs. Development **133:** 251–261.

Scott, R.J., Spielman, M., Bailey, J., and Dickinson, H.G. (1998). Parent-of-origin effects on seed development in *Arabidopsis thaliana*. Development **125:** 3329–3341.

Smaczniak, C., et al. (2012). Characterization of MADS-domain transcription factor complexes in Arabidopsis flower development. Proc. Natl. Acad. Sci. USA **109:** 1560–1565.

Song, X.J., Huang, W., Shi, M., Zhu, M.Z., and Lin, H.X. (2007). A QTL for rice grain width and weight encodes a previously unknown RING-type E3 ubiquitin ligase. Nat. Genet. **39:** 623–630.

Swaminathan, K., Peterson, K., and Jack, T. (2008). The plant B3 superfamily. Trends Plant Sci. **13:** 647–655.

Trigueros, M., Navarrete-Gómez, M., Sato, S., Christensen, S.K., Pelaz, S., Weigel, D., Yanofsky, M.F., and Ferrándiz, C. (2009). The NGATHA genes direct style development in the Arabidopsis gynoecium. Plant Cell **21:** 1394–1409.

Wang, A., Garcia, D., Zhang, H., Feng, K., Chaudhury, A., Berger, F., Peacock, W.J., Dennis, E.S., and Luo, M. (2010). The VQ motif protein IKU1 regulates endosperm growth and seed size in Arabidopsis. Plant J. **63:** 670–679.

Westoby, M., Falster, D.S., Moles, A.T., Vesk, P.A., and Wright, I.J. (2002). Plant ecological strategies: Some leading dimensions of variation between species. Annu. Rev. Ecol. Syst. **33:** 125–159.

Xia, T., Li, N., Dumenil, J., Li, J., Kamenski, A., Bevan, M.W., Gao, F., and Li, Y. (2013). The ubiquitin receptor DA1 interacts with the E3 ubiquitin ligase DA2 to regulate seed and organ size in Arabidopsis. Plant Cell **25:** 3347–3359.

Xiao, W., Brown, R.C., Lemmon, B.E., Harada, J.J., Goldberg, R.B., and Fischer, R.L. (2006). Regulation of seed size by hypomethylation of maternal and paternal genomes. Plant Physiol. **142:** 1160–1168.

Xu, R., and Li, Y. (2011). Control of final organ size by Mediator complex subunit 25 in *Arabidopsis thaliana*. Development **138:** 4545–4554.

Yamasaki, K., et al. (2004). Solution structure of the B3 DNA binding domain of the Arabidopsis cold-responsive transcription factor RAV1. Plant Cell **16:** 3448–3459.

Zhou, Y., Zhang, X., Kang, X., Zhao, X., Zhang, X., and Ni, M. (2009). SHORT HYPOCOTYL UNDER BLUE1 associates with MINISEED3 and HAIKU2 promoters in vivo to regulate Arabidopsis seed development. Plant Cell **21:** 106–117.